

Apigenin ameliorates hypercholesterolemic-induced kidney injury *via* modulating renal *KIM-1*, *Fn1*, and *Nrf2* signaling pathways

S.Y. ALMAGHRABI

Department of Physiology, Faculty of Medicine, King AbdulAziz University, Jeddah, Saudi Arabia

Abstract. – **OBJECTIVE:** Hypercholesterolemia (HC) is a devastating metabolic disorder that has a negative effect on the kidneys' functional and structural modalities *via* oxidative stress and inflammation. The aim of this paper is to elaborate on the role of the flavonoid apigenin (Apg), considering its antioxidant, anti-inflammatory, and antiapoptotic capabilities, in alleviating hypercholesterolemic-induced kidney injury.

MATERIALS AND METHODS: Twenty-four adult Wister male rats were allocated into four equal groups and treated for eight consecutive weeks: a control group, supplemented with a normal pellet diet (NPD); the Apg group, supplemented with NPD and Apg (50 mg/Kg); the HC group, fed with NPD enriched with 4% cholesterol and 2% sodium cholate; and the HC/Apg group, concomitantly rendered hypercholesterolemic and gavaged with Apg. At the end of the experiment, serum samples were collected to measure renal function parameters, lipid profile, MDA, and GPX-1. Thereafter, the kidneys were processed for histological study and homogenized to assess IL-1 β , IL-10, and the gene expression of kidney injury molecule-1 (*KIM-1*), fibronectin 1 (*Fn1*), and NF-E2-related factor 2 (*Nrf2*) *via* RT-qPCR.

RESULTS: HC disturbed the renal function, lipid profile, and serum redox balance. In addition, HC elicited a proinflammatory/anti-inflammatory imbalance, upregulating *KIM-1* and *Fn1* and downregulating the *Nrf2* gene expression of the kidney tissue. Moreover, HC induced marked histopathological changes in the kidney cytoarchitecture. Efficaciously, upon concomitant Apg supplementation with a high-cholesterol diet, most functional, histological, and biomolecular impairments of the kidney were comparatively restored in the HC/Apg group.

CONCLUSIONS: Apg mitigated HC-induced kidney injury *via* modulating the *KIM-1*, *Fn1*, and *Nrf2* signaling pathways, a promising effect that may be useful as an adjunct to antihypercholesterolemic medications to treat the devastating renal complications of HC.

Key Words:

Hypercholesterolemia, Renal injury, Apigenin, *KIM-1*, *Fn1*, *Nrf2*.

Introduction

Cholesterol is an essential compound for the structural integrity of the cell membranes and plays a vital role as a precursor for steroid hormones and bile acids. Elevated blood cholesterol level, known as HC, is a well-established risk factor for cardiovascular, cerebrovascular, and peripheral vascular diseases¹. HC can be defined as LDL cholesterol greater than 190 mg/dL or greater than 160 mg/dL with one major risk factor or greater than 130 mg/dL with two major risk factors. These major risk factors include hypertension, diabetes mellitus, smoking, age (male: 45 years or older; female: 55 years or older), a positive family history of premature atherosclerosis (younger than 55 years in a male and younger than 65 years in a female) and low HDL cholesterol levels (less than 40 mg/dl in male and less than 55 mg/dl in a female)².

HC is mainly due to primary (genetic or familial) or secondary (acquired) causes. The classical genetic disorder is familial hypercholesterolemia due to mutations in the LDL receptor gene, resulting in LDL-C greater than 190 mg/dl in heterozygotes and greater than 450 mg/dl in homozygotes³. These genetic mutations of the LDL receptor gene account for 85% of familial causes. Other genetic causes of familial hypercholesterolemia include defective apolipoprotein B, resulting in a loss of ligands binding to the LDL receptor. Additionally, mutations in the proprotein convertase subtilisin/kexin type 9 (*PCSK9*) gene lead to an increased affinity of *PCSK9* for the LDL receptor, which results in a more rapid clearance of the LDL receptor by targeting it to the lysosome for degradation in the liver, thus resulting in HC²⁻⁶.

All of the above genetic causes are transmitted as autosomal dominant traits. Another rare genetic cause is autosomal recessive hypercholesterolemia due to a mutation in the LDL receptor

adaptor protein, resulting in defective endocytosis of the LDL receptors. However, the most common cause is polygenic HC, which results from an interaction of unidentified genetic factors compounded by a sedentary lifestyle and an increased intake of high saturated fats, trans-fatty acids, and cholesterol²⁻⁶. The acquired causes include diabetes mellitus, cholestatic liver diseases, hypothyroidism, metabolic syndrome, obesity, and nephrotic syndrome. Moreover, some drugs, such as thiazide diuretics, cyclosporine, olanzapine, and smoking have been linked with an increased risk of hypercholesterolemia².

In 2020, the World Health Organization (WHO) revealed the global prevalence of HC to be around 11.9%, accounting for 28.5 million adults aged ≥ 20 years. In Saudi Arabia, the data on the prevalence of hypercholesterolemia are scarce, and the local prevalence ranges widely from 8.5% to 54.9%⁷.

It was hypothesized that, if HC is not promptly treated, many general deleterious effects can be caused, including atherosclerosis, coronary heart disease, myocardial infarction, ischemic cardiomyopathy, sudden cardiac death, ischemic stroke, microvascular disease, erectile dysfunction, and acute limb ischemia⁸.

Determinately, HC is highly prevalent in patients with chronic kidney disease (CKD), and the relation between both issues remains unclearly understood. Hypercholesterolemia is a major risk factor for CKD, owing to HC-induced renal atherosclerosis and OS. It was found that elevated LDL cholesterol is associated with increased systemic levels of oxidized LDL (OxLDL), which is well-known to be involved in endothelial cell dysfunction^{9,10}. Moreover, several experimental studies¹¹ have demonstrated that, in addition to its well-known proatherogenic effect on renal microvasculature, hypercholesterolemia may exacerbate the renal vascular responses to ischemia/reperfusion injury (I/R injury) with subsequent renal dysfunction.

In a crosstalk manner, CKD results in a profound dysregulation of several lipoprotein key enzymes that eventually contributes to increased LDL cholesterol, triglycerides, and triglyceride-rich apolipoprotein B (apoB), together with decreased HDL cholesterol¹². With the progression of CKD, oxidative/nitrative stress participates in renal functional progression¹³⁻¹⁵. Oxidative/nitrative stress is an excess formation or insufficient removal of highly reactive molecules, such as reactive oxygen and/or nitrogen species (ROS and RNS), including superoxide, hydrogen peroxide, hydrox-

yl radical, and peroxynitrite¹⁶. Enzymatic sources for ROS formation include the mitochondrial respiratory chain, nicotinamide adenine dinucleotide phosphate (NADPH) oxidases, xanthine oxidase, cyclooxygenases, uncoupled nitric oxide synthase (NOS), and peroxidases, while antioxidant enzymatic systems include superoxide dismutase (SOD), catalase, glutathione peroxidase, glutathione reductase, and heme oxygenase (HO)¹⁷.

To date, extensive research has been conducted to combat HC. However, no effective and clinically applicable preventive or curative compounds have been established. The major preventive emphasis strategy is directed primarily at exercise and changing lifestyles with strict diet regimens. In addition, several lipid-lowering drugs have been employed, such as statins (HMG-CoA reductase inhibitors), Ezetimibe (inhibits intestinal absorption of cholesterol), and PCSK9 monoclonal antibodies (increases LDL clearance from the circulation)¹⁸. Additionally, Gemcabene (enhances the clearance of VLDLs in plasma and the inhibition of the production of cholesterol and TGs in the liver through its liver-directed downregulation of hepatic apoC-III)¹⁹. Inclisiran increases LDL-C receptor recycling and expression on the hepatocyte cell surface, thereby increasing LDL-C uptake by hepatocytes and lowering LDL-C levels in the bloodstream²⁰. Evinacumab inhibits angiotensin-like 3 (ANGPTL3), which is an inhibitor of lipoprotein and endothelial lipase that is responsible for increasing the levels of triglycerides and other lipids²¹. Vupanorsen reduces the production of the ANGPTL3 protein, which ultimately leads to a reduction in LDL-C levels²². ARO-ANG3 also inhibits ANGPTL3 and is designed to reduce triglycerides and decrease LDL-C in patients with mixed dyslipidemia²³. Bempedoic acid inhibits ATP-citrate lyase, which is a component of the cholesterol synthesis pathway²⁴.

However, the aforementioned synthetic drugs have several deleterious effects, and they are expensive and non-specific. One strategy that holds great promise in combating hypercholesterolemia is the use of flavonoid preparations derived from edible plants. These flavonoids are characterized by exhibiting high antioxidant activity, being well tolerated, cost-effective, of high therapeutic efficacy, and with almost no side effects.

In this study, attention was directed to Apigenin (Apg, one of the promising flavonoids). Apg (4',5,7-trihydroxyflavone) is a natural product belonging to the flavone family and exists principally in vegetables (parsley, celery, and onions), fruits

(oranges), herbs (chamomile, thyme, oregano, and basil), and plant-based beverages²⁵. Apg is used as an alternative regimen with antioxidant, anti-apoptotic, and anti-inflammatory capabilities. Therefore, this study highlights and pays attention to the potentially mitigating role of Apg in the experimentally induced hypercholesterolemia of male rats.

Materials and Methods

Chemicals

All chemicals were purchased from Sigma-Aldrich Co. (St Louis, MO, USA).

Cholesterol: White powder with purity >90% (CAS No: 57-88-5).

Sodium cholate hydrate: (CAS No: 206986-87-0): Dried powder with purity \geq 97.0%.

Apigenin (Apg): Light yellow powder with purity >98% (CAS No: 520-46-5).

Dimethyl Sulfoxide (DMSO): Derived in the form of a clear colorless liquid (CAS No: 76-86-5).

Sodium pentobarbital: A vial of 2 ml solution (Virbac Animal Health, Milperra, NSW, Australia).

Study Setting

This study was conducted at Pharmacology Research Laboratory, Faculty of Pharmacy, King Abdulaziz University, Jeddah, Saudi Arabia, in April-June 2022.

Animals

Adult male Wister rats (n=24, aged approximately 12-16 weeks and weighing 190-220 gm) were used in this study. The rats were obtained from the animal house of the Faculty of Pharmacy, King Abdulaziz University, Jeddah, Saudi Arabia. The rats were left to acclimatize without handling for one week prior to the start of the experiments. The animals were housed in well-ventilated cages at an ambient temperature of 23 ± 2 C°, under the natural 12-hour day/night cycle with free access to a standard commercial rodent chaw and tap water ad libitum throughout the entire study period.

Ethical Statement

The experimental protocol of this study was revised and approved by the local ethical guidelines established by the Research Ethics Committee, Faculty of Pharmacy, King Abdulaziz University, Jeddah, Saudi Arabia (Reference No; PH-1443-18). These institutional rules are in strict accordance with the international guiding principles for the care and use of laboratory animals.

Preparation of the Hypercholesterolemic Diet (HCD)

The rats were kept on two dietary regimens, a standard commercial normal pellet diet (NPD) (for the control group) (Ashirwad Industries, Chandigarh, India) and a hypercholesterolemic diet (HCD) (for the tested groups). The NPD consisted of 48.8% carbohydrates, 21% protein, and 3% fat and 27.2% others (calcium, phosphorus, fibers, and ash). On the other hand, the HCD was reconstituted by enriching the NPD with 4% (weight/weight) cholesterol and 2% (weight/weight) sodium cholate²⁶. All ingredients of the HCD were thoroughly mixed with water and transformed into pellets and then oven-baked at 65 °C overnight for proper drying to avoid fungal contamination. HCD was freshly prepared every 3-4 days and stored at -20°C.

Experimental Groups

The rats were randomly allocated into four groups of six rats each:

- I (Control group): Rats were supplemented with a standard commercial normal pellet diet (NPD) of 48.8% carbohydrates, 21% protein, and 3% fat and 27.2% others (calcium, phosphorus, fibers, and ash) and were gavaged with 0.5 ml DMSO by oral gavage, once daily for eight weeks.
- II (Apg group): This group was supplemented with NPD and gavaged with Apg (50mg/Kg) dissolved in 0.5 ml DMSO by oral gavage, once daily for eight weeks²⁷.
- III (HC group): In this group, the rats were fed orally with NPD enriched with 4% (weight/weight) cholesterol and 2% (weight/weight) sodium cholate for eight weeks²⁶. The development of hypercholesterolemia was confirmed by measuring the serum cholesterol, and rats with cholesterol levels \leq 250 mg/dl were included in the study.
- IV (HC/Apg group): The rats of this group were rendered hypercholesterolemic as in group III for eight weeks; during this time, they were concomitantly gavaged with Apg at the same dose as group II.

Experimental Protocol

At the end of the experiment (after eight weeks), the rats were weighed and fasted overnight. The following day, blood samples were withdrawn from the retro-orbital venous sinuses. The blood samples were left to clot at room temperature in non-heparinized tubes. The collected blood sam-

ples were centrifuged at (3000 rpm. for 15 min) to obtain the serum, which was stored at -20°C until the time of biochemical analysis. Afterward, the rats were weighed and anesthetized using sodium pentobarbital (60 mg/kg) and sacrificed by cervical dislocation. Then, the abdomen was opened by a longitudinal incision, and the left kidney was excised, cleaned from the surrounding fat and connective tissue, and fixed for 48 hours in 10% neutral buffered formalin (NBF) to be processed later for histological study²⁸. The right kidney was excised and homogenized in ice-cold 0.01 M Tris-HCl buffer, pH 7.4, to obtain a 10% homogenate²⁹.

Biochemical Analysis

Measurement of the renal function

Serum urea, creatinine, uric acid, sodium, and potassium were measured. Additionally, the animals were kept for 24 hours in metabolic cages (starting at 08 pm and ending at 08 am the next day), and 24-hour urine samples were collected to measure the level of urinary creatinine. Finally, creatinine clearance was calculated to measure the glomerular filtration rate (GFR).

Measurement of the serum lipid profile

Serum TC, TG, and HDL were analyzed using commercial kits (Nanjing Jiancheng Bioengineering Institute, Nanjing, China). Serum LDL was calculated according to the equation of³⁰ [LDL = TC - (HDL + TG/5)].

Measurement of serum lipid peroxidation and antioxidant enzymes

Malondialdehyde (MDA, an indicator of lipid peroxidation) was determined spectrophotometrically using a thiobarbituric acid reactive substances (TBARS) assay kit (Sigma-Aldrich, Chemical Comp., MO, USA). MDA was expressed as (nmol/ml). In addition, the serum antioxidant enzyme, Glutathione peroxidase-1 (GPX-1), was measured spectrophotometrically using a commercial assay kit (Abcam, UK). GPX-1 was expressed as (U/ml).

Measurement of the renal tissue pro-inflammatory and anti-inflammatory cytokines

In the kidney tissue homogenate, the pro-inflammatory cytokine (IL-1 β) and the anti-inflammatory cytokine (IL-10) were measured using rat ELISA kits following the manufacturer's instructions. IL-1 β and IL-10 were expressed as pg/ μg protein.

Gene Expression Via Real Time-Quantitative Polymerase Chain Reaction (RT-Qpcr)

In the kidney tissue homogenate, the gene expressions of the kidney injury molecule-1 (*KIM-1*), fibronectin 1 (*Fn1*), and NF-E2-related factor 2 (*Nrf2*) were assessed by RT-qPCR. Briefly, the total RNA was extracted from the homogenate using a standard TRIzol RNA isolation method (Invitrogen; Thermo Fisher Scientific, Inc., Waltham, MA, USA); then, cDNA was synthesized using a reverse transcription kit (Reverse Transcriptase Master Mix, Roche Diagnostics) according to the manufacturer's instructions. RT-qPCR analysis was performed in a mixture containing 5 μL cDNA, 10 μL Eva green mix (Jena Bioscience), and 0.6 μL primers (10 μM), with a PCR grade water up to 20 μL . The amplification was carried out using Real-time PCR (Strata gene Mx 3005 P-qPCR System). The amplification conditions were 2 min at 50°C , 10 min at 95°C , and 40 cycles of denaturation for 15 s and annealing/extension at 60°C for 10 min. The relative gene expression of each target cDNA sample relative to the reference sample was calculated. The fold-change of each target gene expression was normalized to the Ct value of a reference gene of glyceraldehyde 3-phosphate dehydrogenase (GAPDH) using the comparative Ct method ($2^{-\Delta\Delta\text{CT}}$) method. The sequence of the primers of the target studied genes and that of GAPDH are shown in Table I.

Histological Study

The formalin-fixed kidneys were dehydrated in ascending grades of ethanol, cleared in xylene, and embedded in paraffin wax; then, serial sections of 5 μm thick were cut using a microtome (Leica RM 2125, Leica Biosystems Nussloch GmbH, Germany)

Table I. Primer sequences of the studied genes for RT qPCR.

Gene	Forward	Reverse
<i>KIM-1</i>	5'-TGGCACTGTGACATCCTCAGA-3'	5'-GCAACGGACATGCCAACATA-3'
<i>Fn1</i>	5'-CTCGCTTTGACTTCACCACCA-3'	5'-TCTCCTTCCTCGCTCAGTTCGACT-3'
<i>Nrf2</i>	5'-CTCTCTGGAGACGGCCATGACT-3'	5'-CTGGGCTGGGGACAGTGGTAGT-3'
<i>GAPDH</i>	5'-TCAAGAAGGTGGTGAAGCAG-3'	5'-AGGTGGAAGAATGGGAGTTG-3'

and mounted on glass slides. Finally, some sections were stained with Hematoxylin and Eosin (H&E) stain “for a routine histological examination of the renal cortex”³¹. Finally, the stained H&E sections were examined under a light microscope.

Statistical Analysis

In the present study, the data were analyzed using the statistical package for social sciences program [SPSS v.23 (IBM, Armonk, NY, USA)] and the GraphPad prism (GraphPad 9 statistical Software, Inc., San Diego, CA, USA). The data are expressed as mean±SD. The variables were checked for normality using Shapiro-Wilk test. The significance of differences between groups was determined by one-way analysis of variance (ANOVA) followed by post-hoc Tukey’s test. *p*-value ≤0.05 was considered statistically significant.

Results

Effect of Apg on the Renal Function

Table II depicts a statistically significant increase in the mean serum urea, uric acid, and creatinine together with a significant decrease in

the creatinine clearance of the HC group compared to that of the control and Apg groups. Upon concomitant Apg administration to the high-cholesterol-fed rats in the HC/Apg group, the deteriorated renal function parameters were returned nearly to a level comparable to that of the control and Apg groups.

Effect of Apg on the Lipid Profile

Table III depicts a statistically significant increase in the mean serum cholesterol, TG, and LDL, together with a significant decrease in serum HDL in the HC group compared to that of the control and Apg groups. In the HC/Apg group, these lipid profile parameters were mitigated compared to those of the HC group.

Effect of Apg on Serum Lipid Peroxidation and Antioxidant Enzymes

There was a statistically significant increase in the mean serum MDA and a decrease in serum GPX-1 in the HC group in comparison with the control and Apg groups. In the HC/Apg group, the mean serum MDA decreased, and serum GPX-1 increased significantly upon concomitant supplementation of Apg with HFD (Table IV).

Table II. Renal function tests in all animal groups (Mean±SD).

	Control group	Apg group	HC group	HC/Apg group	F-test	<i>p</i> -value
Urea (mg/dl)	13.85±0.948	15.70±3.77	76.00±8.50*	34.60±8.44*#	131.4	.000
BUN (mg/dl)	6.46±0.44	7.30±1.73	35.51±3.97*	15.80±3.63*#	135.7	.000
Creatinine (mg/dl)	0.58±0.20	0.56±0.23	2.49±0.57*	1.14±0.34*#	35.4	.000
Creatinine clearance (ml/min)	1.18±0.25	1.15±0.20	0.41±0.14	0.76±0.15	20.5	.000

Values are expressed as Mean±SD of 6 rats of each group. Statistical analysis was carried out using One-way ANOVA followed by Tukey’s test. Statistical significance was set at *p*-value<0.05. *Significant *p*-value when compared to the control group. #Significant *p*-value when compared to the HC group.

Table III. Serum lipid profile in all animal groups (Mean±SD).

	Control group	Apg group	HC group	HC/Apg group	F-test	<i>p</i> -value
Cholesterol (mg/dl)	118.50±5.61	124.16±7.57	292.66±39.08*	193.83±23.6*#	35.1	.000
TG (mg/dl)	75.66±3.9	81.83±6.21	160.33±31.06*	84.50±11.72*#	33.2	.000
HDL (mg/dl)	46.83±3.76	47.33±4.63	23.50±5.64*	37.83±8.03*#	22.5	.000
LDL (mg/dl)	71.66±7.39	76.83±7.44	265.83±45.65*	156.00±30.95*#	33.4	.000

Values are expressed as Mean±SD of 6 rats of each group. Statistical analysis was carried out using One-way ANOVA followed by Tukey’s test. Statistical significance was set at *p*-value <0.05. *Significant *p*-value when compared to the control group. #Significant *p*-value when compared to the HC group.

Table IV. Serum Lipid peroxidation and antioxidant enzymes in all animal groups (Mean±SD).

	Control group	Apg group	HC group	HC/Apg group	F-test	p-value
MDA (nmol/ml)	3.33±0.46	3.08±0.67	14.63±0.77*	70.78±1.13*#	273.3	.000
GPX-1 (U/L)	176.33±10.76	181.33±12.48	86.50±15.57*	175.50±10.78*#	79.4	.000

Values are expressed as Mean±SD of 6 rats of each group. Statistical analysis was carried out using One-way ANOVA followed by Tukey's test. Statistical significance was set at p -value <0.05. *Significant p -value when compared to the control group. #Significant p -value when compared to the HC group.

Effect of Apg on Renal Tissue Pro-Inflammatory and Anti-Inflammatory Cytokines

There was a statistically significant increase in the mean renal tissue IL-1 β and a decrease in IL-10 in the HC group in comparison with the control and Apg groups. In the HC/Apg group, the mean renal tissue IL-1 β decreased and serum IL-10 increased significantly upon concomitant supplementation of Apg with HFD (Table V).

Effect of Apg on the Gene Expression of *KIM-1*, *Fn1*, and *Nrf2* in the Renal Tissue

The results of the qRT-PCR demonstrated that the gene expression of *KIM-1* and *Fn1* increased significantly by ~6-fold, and the expression of *Nrf2* protein decreased by ~10-fold in the kidney tissue of the HC group compared with those of the control and Apg groups. The level of these three renal biomarkers was rescued upon Apg supplementation (Figures 1-3).

Table V. Renal tissue pro-inflammatory and anti-inflammatory cytokines in all animal groups (Mean±SD).

	Control group	Apg group	HC group	HC/Apg group	F-test	p-value
IL-1 β (pg/ μ g protein)	5.96±1.02	5.26±1.58	14.60±0.68*	7.85±0.39#	104.0	.000
IL-10 (pg/ μ g protein)	5.43±1.08	6.23±1.59	2.28±0.84*	13.98±1.81*#	76.8	.000

Values are expressed as Mean±SD of 6 rats of each group. Statistical analysis was carried out using One-way ANOVA followed by Tukey's test. Statistical significance was set at p -value <0.05. *Significant p -value when compared to the control group. #Significant p -value when compared to the HC group.

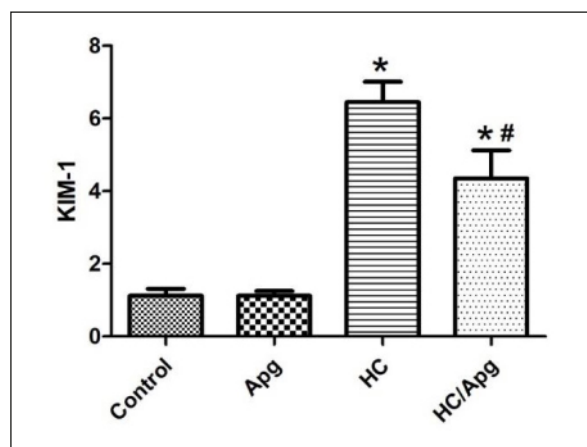


Figure 1. Gene expression of *KIM-1* in the renal tissue in different animal groups (Mean±SD). Values are expressed as Mean±SD of 6 rats of each group. Statistical analysis was carried out using One-way ANOVA followed by Tukey's test. Statistical significance was set at p -value <0.05. *Significant p -value when compared to the control group. #Significant p -value when compared to the HC group.

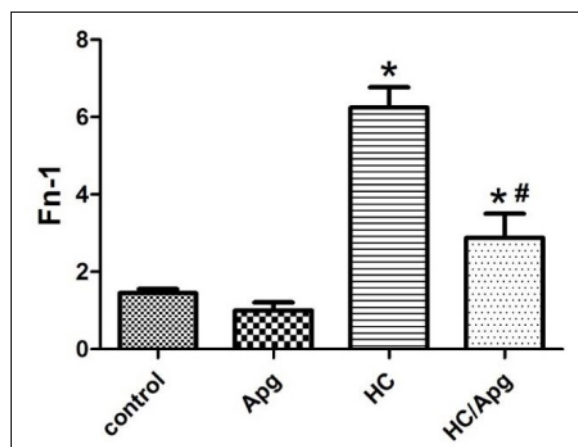


Figure 2. Gene expression of *Fn1* in renal tissue in different animal groups (Mean±SD). Values are expressed as Mean±SD of 6 rats of each group. Statistical analysis was carried out using One-way ANOVA followed by Tukey's test. Statistical significance was set at p -value <0.05. *Significant p -value when compared to the control group. #Significant p -value when compared to the HC group.

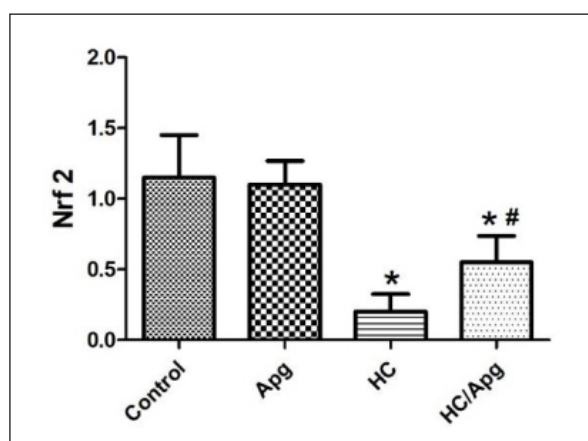


Figure 3. Gene expression of *Nrf2* in renal tissue in different animal groups (Mean±SD). Values are expressed as Mean±SD of 6 rats of each group. Statistical analysis was carried out using One-way ANOVA followed by Tukey's test. Statistical significance was set at p -value<0.05. *Significant p -value when compared to the control group. #Significant p -value when compared to the HC group.

Effect of Apg on the Histology of the Kidney Tissue

The H&E-stained section of the kidney of a control rat (group I) and Apg rat (group II) revealed a normal cytoarchitecture of both cortical and juxtamedullary (JM) nephrons, having renal corpuscles

encompassing normal Bowman's capsule and glomeruli with well-organized juxtaglomerular apparatus. Additionally, both normal proximal convoluted tubules (PT) and distal convoluted tubules (DT) and renal microvasculature were observed (Figures 4-5).

On the other hand, the H&E-stained section in the kidney of the HC rat (group III) displayed sub-capsular congestion and hemorrhage of the renal capsules. Both cortical and JM nephrons exhibited wide Bowman's spaces, dilated congested glomerular capillaries, and a slight expansion of the mesangial matrix. Moreover, dilatated congested microvasculature with focal areas of hemorrhage in the renal interstitium was observed. Additionally, disorganized juxtaglomerular apparatus and dilated congested glomerular afferent and efferent arterioles. The cells of PT and DT were laden with many lipid vacuoles and appeared more acidophilic. The DT showed a dilated lumen with some cells having pyknotic nuclei, and other cells appeared shortened than the control rats (Figure 6).

The H&E-stained section in the kidney of HC/Apg rat (group IV) showed apparently normal cytoarchitecture of both cortical and JM nephrons with an intact visceral layer of Bowman's capsule and the glomerular basement membrane. Moreover, the renal microvasculature revealed mild congestion and minute areas of hemorrhage in the renal interstitium (Figure 7).

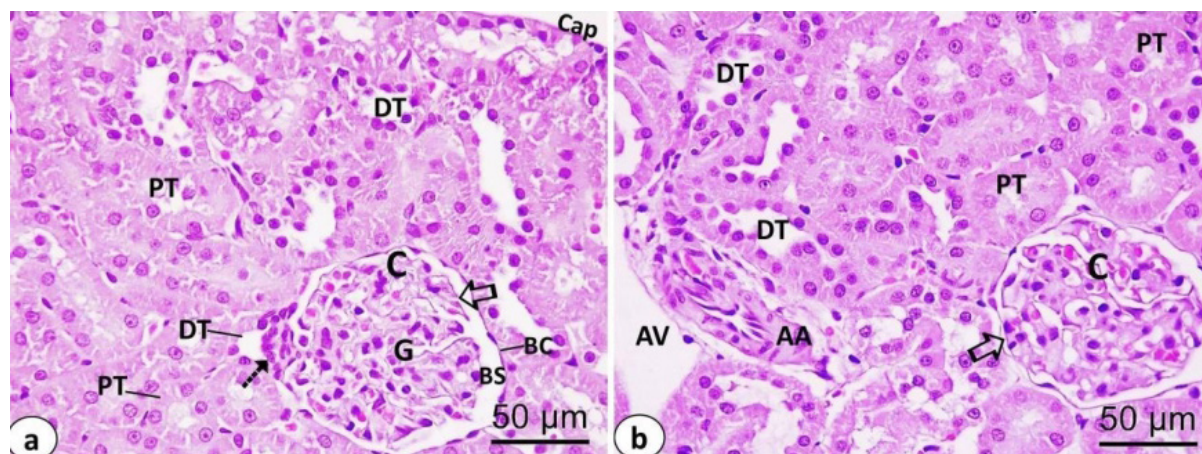


Figure 4. A photomicrograph of the H&E-stained section of the kidney of a control rat. **a**, Normal appearance of the renal capsule (Cap) and cortical nephrons reveal conventional renal corpuscles and renal tubules. The cortical renal corpuscle (C) exhibits Bowman's capsule (BC) with average Bowman's space (BS) and the glomerulus (G), which is in intimate contact with the visceral layer of BC (white arrow). At the vascular pole of the glomerulus, there is a well-organized juxtaglomerular apparatus (interrupted arrow). The cortical renal tubules reveal proximal convoluted tubules (PT) lined by acidophilic tall cuboidal epithelium with a narrow lumen, and distal convoluted tubules (DT) lined by smaller cuboidal epithelium with a wide lumen. **b**, Normal juxtamedullary nephrons with a normal aspect of renal corpuscles and renal tubules. The corpuscle (C) has the same histological features as the cortical corpuscle, with a distinct visceral layer of Bowman's capsule (white arrow). Also, the proximal convoluted tubules (PT) and distal convoluted tubules (DT) appear normal, besides the common arcuate artery (AA) and arcuate vein (AV). Scale bar =50 µm. H&E x400.

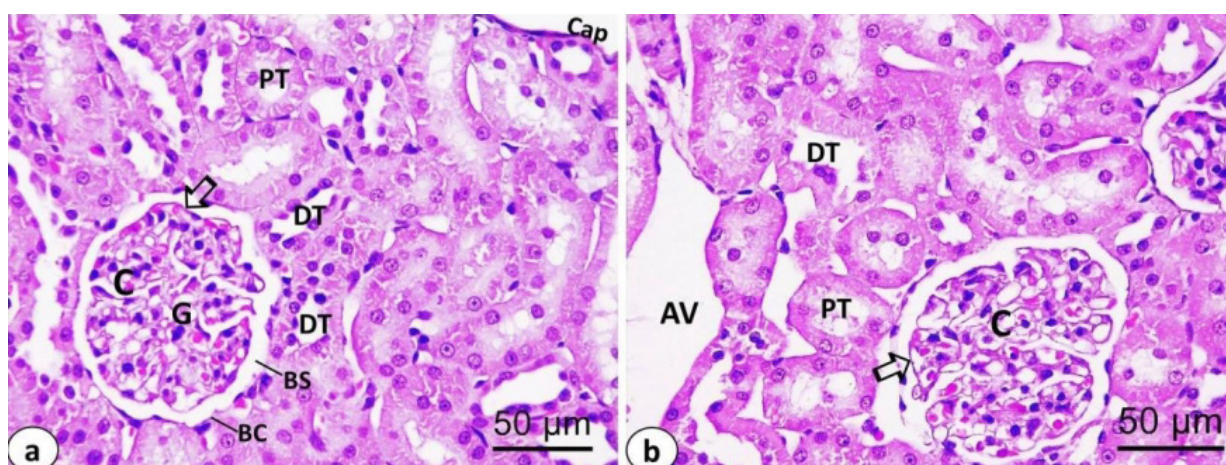


Figure 5. A photomicrograph of the H&E-stained section of the kidney of an Apg-treated rat. **a**, The renal capsule (Cap) and cortical nephrons appear normal. The cortical renal corpuscle (C) exhibits common Bowman's capsule (BC) with average Bowman's space (BS) and the glomerulus (G), which is in intimate contact with the visceral layer of BC (white arrow). The cortical renal tubules reveal regular proximal convoluted tubules (PT) and distal convoluted tubules (DT). **b**, The juxtamedullary nephron exhibits normal renal corpuscle (C) having the same histological appearance as the cortical nephrons with a definite visceral layer of Bowman's capsule (white arrow). Also, PT and DT appear normal, besides the arcuate vein (AV) at the cortico-medullary junction. Scale bar =50µm. H&E x400.

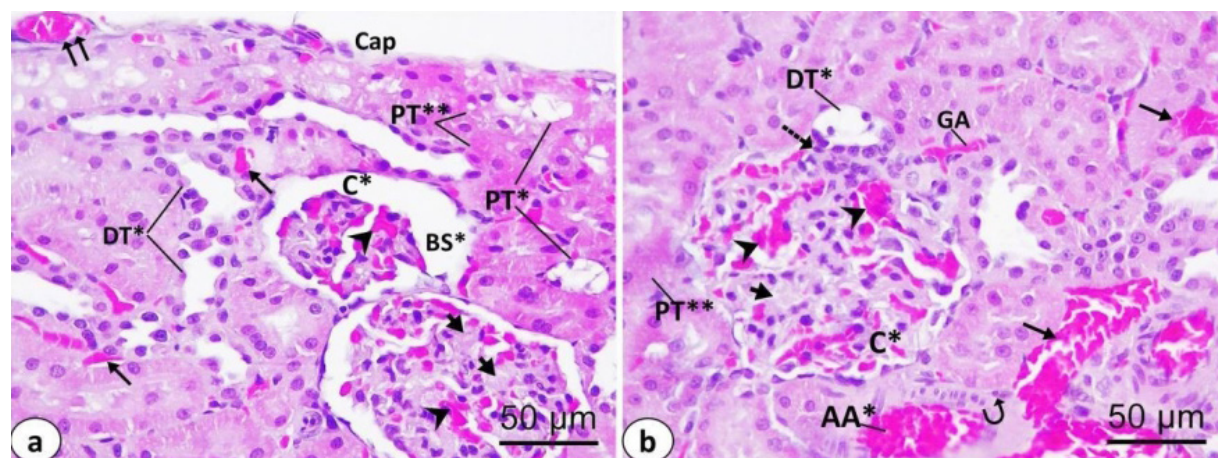


Figure 6. A photomicrograph of the H&E-stained section in the kidney of an HC-treated rat. **a**, A renal capsule (Cap) with subcapsular hemorrhage and congestion (double arrows) are noticed. Also, interstitial vascular congestion with focal areas of hemorrhage (long arrows) is inspected. The cortical nephrons reveal nephropathy, whereas the cortical renal corpuscles (C*) display wide Bowman's space (BS*), dilated congested glomerular capillaries (arrowheads), and a slight expansion of mesangial matrix (short arrows). The cells of some proximal convoluted tubules (PT*) are laden with large lipid vacuoles. The cells of other proximal convoluted tubules (PT**) appear more acidophilic. The distal convoluted tubules (DT*) reveal dilated lumen with some cells having pyknotic nuclei and other cells appear shortened than that of the control rats. **b**, The juxtamedullary nephrons exhibit affected renal corpuscles (C*) that reveal dilated congested glomerular capillaries (arrowheads), and a slight expansion of mesangial matrix (short arrow). Also, disorganized juxtaglomerular apparatus (interrupted arrow). The cells of the distal convoluted tubules (DT*) are loaded with lipid vacuoles alongside dilated congested glomerular arteriole (GA). Some cells of the proximal convoluted tubules appear more acidophilic (PT**). Moreover, dilatation and congestion of the arcuate artery (AA*) with leukocytic infiltration (curved arrow) besides, focal areas of hemorrhage (long arrows) are noticed in the interstitium. Scale bar =50µm. H&E x400.

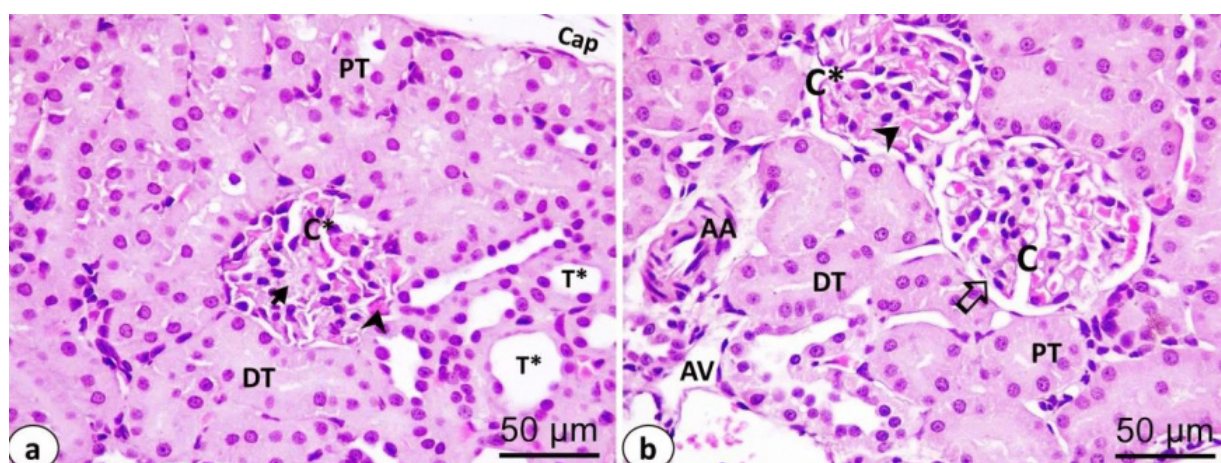


Figure 7. A photomicrograph of the H&E-stained section in the kidney of HC/Apg-treated rat. **a**, The renal capsule (Cap) appears normal without vascular congestion, and the cortical nephrons display an improvement, whereas the renal corpuscles (C*) exhibit slight congestion (arrowhead) in the glomerular capillaries and a minimal proliferation of the mesangial matrix (short arrow). Moreover, some renal tubules (T*) are dilated while the majority of the tubules, proximal (PT) and distal convoluted tubules (DT), are conserved without deposition of fat vacuoles. **b**, The juxtamedullary nephrons illustrate some preserved renal corpuscles (C) with a slightly defined visceral layer of Bowman's capsule with the glomerulus (white arrow), while few renal corpuscles (C*) exhibit slight congestion (arrowhead). However, most of the renal tubules, proximal (PT) and distal convoluted tubules (DT), are preserved. The arcuate artery (AA) and vein (AV) appear normal without congestion. Scale bar = 50µm. H&E x400.

Discussion

Hypercholesterolemia (HC) is a metabolic disorder that increases the risk of renal diseases. The renal burden depends on the degree and duration of exposure to raised cholesterol levels. In this study, the rats supplemented with a high-cholesterol diet (HC group) had oxidative stress (OS) that was intermingled with disturbed biomarkers of oxidant/antioxidant balance, whereby the serum MDA, a marker of lipid peroxidation product, increased, while the serum GPX-1 activity decreased in the HC rats. It was reported that HC caused the oxidative modification of LDL, protein glycation, and glucose-auto-oxidation, thus leading to an excess production of lipid peroxidation products, particularly MDA, which may cause an elevation of OS in hyperlipidemic subjects^{32,33}. Equivalently, it was found that MDA increased in the renal tissue of hypercholesterolemic rats³⁴. Additionally, HC is known to induce OS through the activation of xanthine oxidase, which combines with xanthine to generate reactive oxygen species (ROS)^{35,36}. Moreover, Green et al³⁷ have found that diet-induced hypercholesterolemia increased ROS levels, contributing secondarily to a decrease in the peroxidase activity of the enzymatic antioxidant glutathione in rats.

Previous studies³⁸⁻⁴⁰ have shown that HC is an independent risk factor for the onset and progression of renal disease *via* the induction of OS in the kidneys. This effect of the HC diet added a pro-oxidant burden to the naturally occurring one in the kidneys due to its intertwined renal vasculature that often causes renal ischemia-reperfusion injury (IRI) with the subsequent production of overwhelming ROS, which are common mediators underlying various kidney diseases³⁹. In line with this, patients with chronic kidney disease (CKD) often experience an imbalance between oxygen reactive species (ROS) production and antioxidant defenses, leading to cell and tissue damage⁴⁰. Earlier studies⁴¹ have shown a positive correlation between the imbalance in pro-oxidant and antioxidant activities and renal dysfunction in humans. Strikingly, OS has been found even in the early stages of CKD, and it seems to increase as CKD progresses and correlates significantly and inversely with the level of glomerular filtration rate (GFR) as reflected by an increased systemic marker of OS plasma 8-isoprostane levels⁴². Additionally, Witko-Sarsat et al⁴³ found the same results using other markers of OS, including MDA and GPX.

Therefore, the modulation of HC-induced renal OS is a feasible approach to prevent and/or treat deleterious renal consequences. This mod-

ulation can be approached in at least three different ways. First, cholesterol-lowering therapies have indirect secondary antioxidant properties. Second, the induction of endogenous enzymatic antioxidant systems or the inhibition of the prooxidant enzymes may be feasible. The third novel approach is the application of antioxidant molecules, particularly those of natural products such as flavonoids⁸.

In this regard, the third approach was chosen in this study, where the concomitant administration of the flavonoid Apigenin (Apg) alongside the high-cholesterol diet could successfully mitigate the oxidant/antioxidant imbalance and restore the MDA and GPX-1 to approximately their basal control levels. Many studies^{44,45} have reported the antioxidant activity of Apg. Recently, an *in vitro* study⁴⁴ and another *in vivo* study⁴⁵ have documented an efficacious antioxidant activity of Apg against renal tubular epithelial cell injury.

In this study, the obtained HC-induced redox imbalance may be beyond the histoarchitecture changes that were clearly contemplated under the light microscopic examination of the kidney tissue. Obviously, microscopic changes involving both glomeruli and renal tubules of the cortical and juxtamedullary nephrons were observed and pointed mostly to the development of glomerulosclerosis and segmental necrosis in the renal tissues of the HC group. Moreover, dilatation in glomerular capillaries and Bowman's space were detected; in addition, many necrotic interstitial cells in the kidneys of the HC rats were observed. The aforementioned renal histopathological changes were partially ameliorated in HC/Apg group.

Redox imbalance and inflammation of the renal tissue was encountered in HC rats where a significant concomitant increase in pro-inflammatory markers (IL-1 β) and a decrease in the anti-inflammatory markers (IL-10) in the renal tissue homogenate of the HC group was detected compared with those of the control one. Based on the histological evidence, the inflammation of the renal tissue in the HC group was evident and confirmed under a light microscope, where mononuclear cell infiltration in the renal cortices was contemplated. Inflammatory cells, which are locally activated in the renal microenvironment or migrate from hematopoietic organs, further produce ROS. Thus, the crosstalk between OS and inflammation represents a key aggravating factor for the initiation and progression of acute kidney diseases, including diabetic nephropathy, hypertension-associated kidney disease, and toxic-induced nephropathy³⁹.

Pathologically, HC represents an inconvenience mechanism that drives the associated renal injury. The high-cholesterol diet frequently known as the western diet (WD), which is characterized by highly processed foods with high fat content, is one of the major contributors to the increased incidence of CKD⁴⁶. Population-based studies⁴⁷ have determined that high cholesterol is a strong independent risk factor for end-stage renal disease (ESRD), even after adjusting for other major risk factors associated with this condition.

Comparatively, the HC/Apg group of rats exhibited a significant drop in IL-1 β and a rise in IL-10 in the renal tissue homogenate, a distinctive finding that implies the anti-inflammatory capability of Apg. In previous studies^{48,49}, Apg has shown several valuable bioactive properties, such as antioxidant and anti-inflammatory activities. Apg has been repeatedly reported to attenuate the nephrotoxicity caused by several toxic agents *via* its antioxidant and anti-inflammatory attributes^{44,50,51}.

In this work, in conjunction with the renal tissue inflammation, a derangement of the lipid profile was encountered in HC rats where there was a significant increase in serum cholesterol and triglyceride, and LDL, together with a decrease in HDL. This HC-associated dyslipidemia worsened the renal function biomarkers with a rise in serum urea, BUN, and creatinine aligned with decreased GFR as employed by decreased creatinine clearance. These findings might point to the possibility of the development of CKD following a chronic high-cholesterol diet.

As part of a vicious circle, all patients with CKD experience a secondary form of dyslipidemia characterized by increased serum triglycerides with elevated VLDL, small dense LDL particles, and low HDL cholesterol. All these particles are characterized by triglyceride-rich apolipoprotein B (apoB)-containing complex lipoproteins, which have a significant atherogenic potential⁵². CKD results in the profound dysregulation of several key enzymes and metabolic pathways that eventually contributes to dyslipidemia. With the progression of CKD, these metabolic derangements may be further worsened and participate in atherogenic diathesis and possibly further progression of renal dysfunction¹⁴.

Previous animal studies⁵³⁻⁵⁵ have shown a positive correlation between the presence of an atherogenic lipid profile and the onset of glomerulosclerosis and endothelial dysfunction. In this respect, disrupted lipid profile, kidney function, and structure were employed in diet-induced hypercholesterolemia in both rat models^{55,56} and mice mod-

els^{57,58}. Consistent with the experimental models, dyslipidemia in humans is usually associated with the development and progression of renal dysfunction⁵⁹. Among human studies relating dyslipidemia to the renal outcome, one study⁵⁹ found that a higher total cholesterol and a lower HDL cholesterol were significantly associated with an increased risk of developing renal dysfunction.

In this study, Apg significantly restored the distorted lipid profile upon its concomitant supplementation with 4% cholesterol and 2% sodium cholate. Inconsistent with these results, Apg regulated cholesterol metabolism *in vivo* and antilipidemic effect^{60,61}. Moreover, Apg improved lipid metabolism *in vitro*⁶². These collective results shifted the attention gradually in recent years to Apg as a novel antilipidemic natural plant flavonoid with a high efficacy and few adverse effects rather than the available antilipidemic drugs.

Profound dyslipidemia in the HC group could explain the accumulation of fat droplets in the renal tubules upon the light microscopic examination of the kidney tissue. This finding was in line with a previous work in which HC caused the accumulation of fat droplets in the tubular cells of rats⁶³. The accumulation of fat droplets in tubular cells initiated lipotoxicity that determinately affects the cell metabolism with the overproduction of OS and increased cell apoptosis⁶⁴. Szeto et al⁶⁵ have shown that excess fat droplets in the kidney lead to mitochondrial damage in all renal cell types, with 50% cell loss, reduced size, and loss of cristae membranes that contain the protein complexes of the electron transport chain; thus, a loss of ATP production was employed. Another drawback of excess fat droplets in the kidney is an increased inflammatory cell infiltration in the histological analysis of the kidney tissue⁶³. Indistinguishably, this drawback was strikingly achieved in this study.

The disclosed HC-induced lipid accumulation in the kidney tissue was associated with an increased expression of the immune-related biomarkers genes, viz., kidney injury molecule-1 (*KIM-1*) and fibronectin 1 (*Fnl*), in the renal tissue of the HC group. Biologically, *KIM-1* is a type 1 transmembrane protein that serves as a urinary marker in acute renal tubular injury⁶⁶. In a human study⁶⁷, high urinary *KIM-1* levels and an extensive expression of this protein were detected in biopsies from the proximal tubule of patients with acute tubular necrosis. In a somewhat analogous manner to *KIM-1*, fibronectin 1 (*Fnl*) is an extracellular matrix protein that is linked to some renal diseases characterized by proteinuria, hematuria,

and considerable fibronectin deposits in the mesangium and subendothelial space, subsequently leading to end-stage renal failure⁶⁸. Upregulated *Fnl* gene has been identified in several human diseases, including renal carcinoma. In previous studies^{69,70}, *Fnl* mRNA expression was significantly higher in renal cell carcinoma (RCC) compared to that in normal renal tissue, indicating its possible role in renal carcinogenesis and its progression. Recently, it has been intriguing to speculate that the ubiquitous expression of *Fnl* is an unfortunate common histological endpoint of progressive CKD⁷¹.

Another critical gene that was unfortunately downregulated in the kidney tissue of the HC group was the transcription factor *Nrf2*. This factor normally serves to protect the cells from harmful oxidative stress, playing an integrative role in inducing the expression of genes encoding enzymes involved in antioxidant (e.g., glutathione and NADPH) production and the reduction in pro-oxidants (e.g., heme and quinonoids)³⁹. It was determined that the loss of *Nrf2* aggravates tissue damage and fibrosis in kidney disease models, such as autoimmune nephritis⁷², diabetic nephropathy⁷³, toxic injury⁷⁴, and IRI⁷⁵. Additionally, clinical trials investigating *Nrf2*-activating compounds in kidney disease patients are ongoing, and beneficial effects are being obtained³⁹. Successfully, Apg modulated the HC-induced *KIM-1*, *Fnl*, and *Nrf2* gene expression in the kidney tissue.

Limitations

We acknowledge that this study has some limitations. Kidney function in rats could not be assessed *via* monitoring the passage of an extracellular contrast agent in conjunction with MRI, which is a gold standard method that could enable us to better understand the relative contributions of HC to the detrimental renal functional outcomes and subtle structural abnormalities, as it is not available in our lab.

Conclusions

The results reveal that Apg ameliorated HC-induced renal injury by suppressing not only oxidative stress and inflammation, but also it has a beneficial role in modulating the HC-induced *KIM-1*, *Fnl*, and *Nrf2* gene expression. Therefore, Apg is expected to emerge as a first-in-class innovative natural flavonoid strategy for preventing HC-induced kidney injury and its future transfer to clinical applications must be a paramount concern.

Acknowledgments

The author would like to express her appreciation and special thanks to Professor Mohamed Bendary, Physiology Department, Faculty of Medicine, King Abdulaziz University.

Funding

This research received no external funding.

ORCID ID

Safa Yousef Almaghrabi: 0000-0001-5713-6732

Conflicts of Interests

The author declares no competing interests.

Availability of Data and Materials

The data supporting this study's findings are available from the author.

Ethics Approval

The experimental protocol of this study was revised and approved by the local ethical guidelines established by the Research Ethics Committee, Faculty of Pharmacy, King Abdulaziz University, Jeddah, Saudi Arabia (Reference No; PH-1443-18). These institutional rules are in strict accordance with the international guiding principles for the care and use of laboratory animals.

References

- 1) Durrington P. Dyslipidaemia. *Lancet* 2003; 362: 717-731.
- 2) Ibrahim MA, Asuka E, Jialal I. Hypercholesterolemia. In: *StatPearls*. Treasure Island (FL): StatPearls Publishing LLC; 2022.
- 3) Mytilinaiou M, Kyrou I, Khan M, Grammatopoulos DK, Randeve HS. Familial hypercholesterolemia: New horizons for diagnosis and effective management. *Front Pharmacol* 2018; 9: 707.
- 4) Sturm AC, Knowles JW, Gidding SS, Ahmad ZS, Ahmed CD, Ballantyne CM, Baum SJ, Bourbon M, Carrie A, Cuchel M, de Ferranti SD, Defesche JC, Freiburger T, Hershberger RE, Hovingh GK, Karayan L, Kastelein JJP, Kindt I, Lane SR, Leigh SE, Linton MF, Mata P, Neal WA, Nordestgaard BG, Santos RD, Harada-Shiba M, Sijbrands EJ, Stitziel NO, Yamashita S, Wilemon KA, Ledbetter DH, Rader DJ. Convened by the Familial Hypercholesterolemia Foundation. Clinical genetic testing for familial hypercholesterolemia: JACC scientific expert panel. *J Am Coll Cardiol* 2018; 72: 662-680.
- 5) Alaqeel A, Alrashidi A. Gaps in knowledge and practice for familial hypercholesterolemia among physicians caring for children in Saudi Arabia. *Eur Rev Med Pharmacol Sci* 2022; 26: 2727-2739.
- 6) Li G, Wu X, Kong X, Wang L, Jin X. Cytochrome c oxidase subunit VIIb as a potential target in familial hypercholesterolemia by bioinformatical analysis. *Eur Rev Med Pharmacol Sci* 2015; 19: 4139-4145.
- 7) Al-Zahrani J, Shubair MM, Al-Ghamdi S, Alrashied AA, Alduraywish AA, Alreshidi FS, Alshahrani SM, Alsalamah M, Al-Khateeb BF, Ashathri AI, El-Metwally A, Aldossari KK. The prevalence of hypercholesterolemia and associated risk factors in al-kharj population, Saudi Arabia: A cross-sectional survey. *BMC Cardiovasc Disord* 2021; 21: 22-2.
- 8) Csonka C, Sarkozy M, Pipicz M, Dux L, Csont T. Modulation of hypercholesterolemia-induced oxidative/nitrative stress in the heart. *Oxid Med Cell Longev* 2016; 2016: 3863726.
- 9) Duarte MM, Rocha JB, Moresco RN, Duarte T, Da Cruz IB, Loro VL, Schetinger MR. Association between ischemia-modified albumin, lipids and inflammation biomarkers in patients with hypercholesterolemia. *Clin Biochem* 2009; 42: 666-671.
- 10) Raman KG, Gandley RE, Rohland J, Zenati MS, Tzeng E. Early hypercholesterolemia contributes to vasomotor dysfunction and injury associated atherogenesis that can be inhibited by nitric oxide. *J Vasc Surg* 2011; 53: 754-763.
- 11) Stokes KY, Granger DN. Hypercholesterolemia: Its impact on ischemia-reperfusion injury. *Expert Rev Cardiovasc Ther* 2005; 3: 1061-1070.
- 12) Vaziri ND, Norris K. Lipid disorders and their relevance to outcomes in chronic kidney disease. *Blood Purif* 2011; 31: 189-196.
- 13) Trevisan R, Dodesini AR, Lepore G. Lipids and renal disease. *J Am Soc Nephrol* 2006; 17: 145.
- 14) Vaziri ND. Dyslipidemia of chronic renal failure: The nature, mechanisms, and potential consequences. *Am J Physiol Renal Physiol* 2006; 290: 262.
- 15) Vaziri ND, Moradi H. Mechanisms of dyslipidemia of chronic renal failure. *Hemodial Int* 2006; 10: 1-7.
- 16) Halliwell B. Biochemistry of oxidative stress. *Biochem Soc Trans* 2007; 35: 1147-1150.
- 17) Droge W. Free radicals in the physiological control of cell function. *Physiol Rev* 2002; 82: 47-95.
- 18) Ference BA, Ginsberg HN, Graham I, Ray KK, Packard CJ, Bruckert E, Hegele RA, Krauss RM, Raal FJ, Schunkert H, Watts GF, Boren J, Fazio S, Horton JD, Masana L, Nicholls SJ, Nordestgaard BG, van de Sluis B, Taskiran MR, Tokgozlu L, Landmesser U, Laufs U, Wiklund O, Stock JK, Chapman MJ, Catapano AL. Low-density lipoproteins cause atherosclerotic cardiovascular disease. 1. evidence from genetic, epidemiologic, and clinical studies. A consensus statement from the European Atherosclerosis Society consensus panel. *Eur Heart J* 2017; 38: 2459-2472.

- 19) Stein E, Bays H, Koren M, Bakker-Arkema R, Bisgaier C. Efficacy and safety of gemcabene as add-on to stable statin therapy in hypercholesterolemic patients. *J Clin Lipidol* 2016; 10: 1212-1222.
- 20) Ray KK, Wright RS, Kallend D, Koenig W, Leiter LA, Raal FJ, Bisch JA, Richardson T, Jaros M, Wijngaard PLJ, Kastelein JJP, ORION-10 and ORION-11 Investigators. Two phase 3 trials of inclisiran in patients with elevated LDL cholesterol. *N Engl J Med* 2020; 382: 1507-1519.
- 21) Raal FJ, Rosenson RS, Reeskamp LF, Hovingh GK, Kastelein JJP, Rubba P, Ali S, Banerjee P, Chan KC, Gipe DA, Khilla N, Pordy R, Weinreich DM, Yancopoulos GD, Zhang Y, Gaudet D, ELIPSE HoFH Investigators. Evinacumab for homozygous familial hypercholesterolemia. *N Engl J Med* 2020; 383: 711-720.
- 22) Jia X, Al Rifai M, Hussain A, Martin S, Agarwala A, Virani SS. Highlights from studies in cardiovascular disease prevention presented at the digital 2020 european society of cardiology congress: Prevention is alive and well. *Curr Atheroscler Rep* 2020; 22: 72.
- 23) Tromp TR, Stroes ESG, Hovingh GK. Gene-based therapy in lipid management: The winding road from promise to practice. *Expert Opin Investig Drugs* 2020; 29: 483-493.
- 24) Laufs U, Banach M, Mancini GBJ, Gaudet D, Bloedon LT, Sterling LR, Kelly S, Stroes ESG. Efficacy and safety of bempedoic acid in patients with hypercholesterolemia and statin intolerance. *J Am Heart Assoc* 2019; 8: e011662.
- 25) Hostetler GL, Ralston RA, Schwartz SJ. Flavones: Food sources, bioavailability, metabolism, and bioactivity. *Adv Nutr* 2017; 8: 423-435.
- 26) Kasiske BL, O'Donnell MP, Schmitz PG, Kim Y, Keane WF. Renal injury of diet-induced hypercholesterolemia in rats. *Kidney Int* 1990; 37: 880-891.
- 27) Kang HK, Ecklund D, Liu M, Datta SK. Apigenin, a non-mutagenic dietary flavonoid, suppresses lupus by inhibiting autoantigen presentation for expansion of autoreactive Th1 and Th17 cells. *Arthritis Res Ther* 2009; 11: R59.
- 28) Matsuo T, Ishikawa E, Ohta M, Shibouta Y, Ishimura Y, Imura Y, Sugiyama Y. Renal protective effect of candesartan cilexetil in spontaneously hypercholesterolemic rats. *Jpn J Pharmacol* 2002; 88: 300-306.
- 29) Sudhakar V, Ashok Kumar S, Varalakshmi P, Sujatha V. Protective effect of lupeol and lupeol linoleate in hypercholesterolemia associated renal damage. *Mol Cell Biochem* 2008; 317: 11-20.
- 30) Friedewald WT, Levy RI, Fredrickson DS. Estimation of the concentration of low-density lipoprotein cholesterol in plasma, without use of the preparative ultracentrifuge. *Clin Chem* 1972; 18: 499-502.
- 31) Bancroft JD and Layton C. The hematoxylin and eosin. In: Churchill Livingstone Elsevier; 2013: 179-220.
- 32) Prasad K, Lee P. Suppression of hypercholesterolemic atherosclerosis by pentoxifylline and its mechanism. *Atherosclerosis* 2007; 192: 313-322.
- 33) Yang RL, Shi YH, Hao G, Li W, Le GW. Increasing oxidative stress with progressive hyperlipidemia in human: Relation between malondialdehyde and atherogenic index. *J Clin Biochem Nutr* 2008; 43: 154-158.
- 34) Minami M, Ishiyama A, Takagi M, Omata M, Atarashi K. Effects of allopurinol, a xanthine oxidase inhibitor, on renal injury in hypercholesterolemia-induced hypertensive rats. *Blood Press* 2005; 14: 120-125.
- 35) Daghini E, Chade AR, Krier JD, Versari D, Lerman A, Lerman LO. Acute inhibition of the endogenous xanthine oxidase improves renal hemodynamics in hypercholesterolemic pigs. *Am J Physiol Regul Integr Comp Physiol* 2006; 290: 609.
- 36) Scheuer H, Gwinner W, Hohbach J, Grone EF, Brandes RP, Malle E, Olbricht CJ, Walli AK, Grone HJ. Oxidant stress in hyperlipidemia-induced renal damage. *Am J Physiol Renal Physiol* 2000; 278: 63.
- 37) Green CO, Wheatley AO, McGrowder DA, Dilworth LL, Nosakhare Asemota H. Modulation of antioxidant enzymes activities and lipid peroxidation products in diet-induced hypercholesterolemic rats fed ortanique peel polymethoxylated flavones extract. *Journal of Applied Biomedicine* 2012; 10: 91-101.
- 38) Prasad K. Vitamin E and regression of hypercholesterolemia-induced oxidative stress in kidney. *Mol Cell Biochem* 2014; 385: 17-21.
- 39) Nezu M, Suzuki N. Roles of Nrf2 in protecting the kidney from oxidative damage. *Int J Mol Sci* 2020; 21: 2951.
- 40) Poulianiti KP, Kaltsatou A, Mitrou GI, Jamurtas AZ, Koutedakis Y, Maridaki M, Stefanidis I, Sakkas GK, Karatzaferi C. Systemic redox imbalance in chronic kidney disease: A systematic review. *Oxid Med Cell Longev* 2016; 2016: 8598253.
- 41) Tepel M, Echelmeyer M, Orrie NN, Zidek W. Increased intracellular reactive oxygen species in patients with end-stage renal failure: Effect of hemodialysis. *Kidney Int* 2000; 58: 867-872.
- 42) Dounousi E, Papavasiliou E, Makedou A, Ioannou K, Katopodis KP, Tselepis A, Siamopoulos KC, Tsakiris D. Oxidative stress is progressively enhanced with advancing stages of CKD. *Am J Kidney Dis* 2006; 48: 752-760.
- 43) Witko-Sarsat V, Friedlander M, Nguyen Khoa T, Capeillere-Blandin C, Nguyen AT, Canteloup S, Dayer JM, Jungers P, Druke T, Descamps-Latscha B. Advanced oxidation protein products as novel mediators of inflammation and monocyte activation in chronic renal failure. *J Immunol* 1998; 161: 2524-2532.
- 44) Zhang J, Zhao X, Zhu H, Wang J, Ma J, Gu M. Apigenin protects against renal tubular epithelial cell injury and oxidative stress by high glucose via

- regulation of NF-E2-related factor 2 (Nrf2) pathway. *Med Sci Monit* 2019; 25: 5280-5288.
- 45) Wu Q, Li W, Zhao J, Sun W, Yang Q, Chen C, Xia P, Zhu J, Zhou Y, Huang G, Yong C, Zheng M, Zhou E, Gao K. Apigenin ameliorates doxorubicin-induced renal injury via inhibition of oxidative stress and inflammation. *Biomed Pharmacother* 2021; 137: 111308.
 - 46) Odermatt A. The western-style diet: A major risk factor for impaired kidney function and chronic kidney disease. *Am J Physiol Renal Physiol* 2011; 301: 919.
 - 47) Nguyen S, Hsu CY. Excess weight as a risk factor for kidney failure. *Curr Opin Nephrol Hypertens* 2007; 16: 71-76.
 - 48) Arango D, Dios-Toro M, Rojas-Hernandez LS, Cooperstone JL, Schwartz SJ, Mo X, Jiang J, Schmittgen TD, Doseff AI. Dietary apigenin reduces LPS-induced expression of miR-155 restoring immune balance during inflammation. *Mol Nutr Food Res* 2015; 59: 763-772.
 - 49) Nabavi SF, Khan H, D'onofrio G, Šamec D, Shirooie S, Dehpour AR, Argüelles S, Habtemariam S, Sobarzo-Sanchez E. Apigenin as neuroprotective agent: Of mice and men. *Pharmacological research* 2018; 128: 359-365.
 - 50) Ahmad A, Kumari P, Ahmad M. Apigenin attenuates edifenphos-induced toxicity by modulating ROS-mediated oxidative stress, mitochondrial dysfunction and caspase signal pathway in rat liver and kidney. *Pestic Biochem Physiol* 2019; 159: 163-172.
 - 51) Hassan SM, KhalafMM, Sadek SA, Abo-Youssef AM. Protective effects of apigenin and myricetin against cisplatin-induced nephrotoxicity in mice. *Pharmaceutical Biology* 2017; 55: 766-774.
 - 52) Vaziri ND. Molecular mechanisms of lipid disorders in nephrotic syndrome. *Kidney Int* 2003; 63: 1964-1976.
 - 53) Chen HC, Guh JY, Shin SJ, Lai YH. Pravastatin suppress superoxide and fibronectin production of glomerular mesangial cells induced by oxidized-LDL and high glucose. *Atherosclerosis* 2002; 160: 141-146.
 - 54) Vazquez-Perez S, Aragoncillo P, de Las Heras N, Navarro-Cid J, Cediel E, Sanz-Rosa D, Ruilope LM, Diaz C, Hernandez G, Lahera V, Cachofeiro V. Atorvastatin prevents glomerulosclerosis and renal endothelial dysfunction in hypercholesterolaemic rabbits. *Nephrol Dial Transplant* 2001; 16 Suppl 1: 40-44.
 - 55) Wang Z, Huang W, Li H, Tang L, Sun H, Liu Q, Zhang L. Synergistic action of inflammation and lipid dysmetabolism on kidney damage in rats. *Ren Fail* 2018; 40: 175-182.
 - 56) Albrahim T. Lycopene modulates oxidative stress and inflammation in hypercholesterolemic rats. *Pharmaceuticals (Basel)* 2022; 15: 1420.
 - 57) Orsolich N, Landeka Jurcevic I, Dikic D, Rogic D, Odeh D, Balta V, Perak Junakovic E, Terzic S, Jutric D. Effect of propolis on diet-induced hyperlipidemia and atherogenic indices in mice. *Antioxidants (Basel)* 2019; 8: 156.
 - 58) Yang Y, Sun Q, Xu X, Yang X, Gao Y, Sun X, Zhao Y, Ding Z, Ge W, Cheng R, Zhang J. Oral administration of succinoglycan riclin improves diet-induced hypercholesterolemia in mice. *J Agric Food Chem* 2019; 67: 13307-13317.
 - 59) Schaeffner ES, Kurth T, Curhan GC, Glynn RJ, Rexrode KM, Baigent C, Buring JE, Gaziano JM. Cholesterol and the risk of renal dysfunction in apparently healthy men. *Journal of the American Society of Nephrology* 2003; 14: 2084-2091.
 - 60) Lu J, Meng Z, Cheng B, Liu M, Tao S, Guan S. Apigenin reduces the excessive accumulation of lipids induced by palmitic acid via the AMPK signaling pathway in HepG2 cells. *Exp Ther Med* 2019; 18: 2965-2971.
 - 61) Zhang K, Song W, Li D, Jin X. Apigenin in the regulation of cholesterol metabolism and protection of blood vessels. *Exp Ther Med* 2017; 13: 1719-1724.
 - 62) Ren B, Qin W, Wu F, Wang S, Pan C, Wang L, Zeng B, Ma S, Liang J. Apigenin and naringenin regulate glucose and lipid metabolism and ameliorate vascular dysfunction in type 2 diabetic rats. *Eur J Pharmacol* 2016; 773: 13-23.
 - 63) Altunkaynak ME, Özbek E, Altunkaynak BZ, Can İ, Unal D, Unal B. The effects of high-fat diet on the renal structure and morphometric parametric of kidneys in rats. *Journal of anatomy* 2008; 212: 845-852.
 - 64) Balarini CM, Oliveira MZ, Pereira TM, Silva NF, Vasquez EC, Meyrelles SS, Gava AL. Hypercholesterolemia promotes early renal dysfunction in apolipoprotein E-deficient mice. *Lipids Health Dis* 2011; 10: 220-220.
 - 65) Szeto HH, Liu S, Soong Y, Alam N, Prusky GT, Seshan SV. Protection of mitochondria prevents high-fat diet-induced glomerulopathy and proximal tubular injury. *Kidney Int* 2016; 90: 997-1011.
 - 66) Peng S, Liu N, Wei K, Li G, Zou Z, Liu T, Shi M, Lv Y, Lin Y. The predicted value of kidney injury molecule-1 (KIM-1) in healthy people. *Int J Gen Med* 2022; 15: 4495-4503.
 - 67) Han WK, Bailly V, Abichandani R, Thadhani R, Bonventre JV. Kidney injury molecule-1 (KIM-1): A novel biomarker for human renal proximal tubule injury. *Kidney Int* 2002; 62: 237-244.
 - 68) Strøm EH, Banfi G, Krapf R, Abt AB, Mazzucco G, Monga G, Gloor F, Neuweiler J, Riess R, Stosiek P, Hebert LA, Sedmak DD, Gudat F, Mihatsch MJ. Glomerulopathy associated with predominant fibronectin deposits: A newly recognized hereditary disease. *Kidney International* 1995; 48: 163-170.
 - 69) Steffens S, Schrader AJ, Vetter G, Eggers H, Blasig H, Becker J, Kuczyk MA, Serth J. Fibronectin 1 protein expression in clear cell renal cell carcinoma. *Oncol Lett* 2012; 3: 787-790.
 - 70) Waalkes S, Atschekzei F, Kramer MW, Hennenlotter J, Vetter G, Becker JU, Stenzl A, Merseburger AS, Schrader AJ, Kuczyk MA, Serth J. Fibronectin 1 mRNA expression correlates with advanced disease in renal cancer. *BMC Cancer* 2010; 10: 503-503.

- 71) Skoczynski K, Kraus A, Buettner-Herold M, Amann K, Schiffer M, Hermann K, Herrnberger L, Tamm E, Buchholz B. The extracellular matrix protein fibronectin modulates metanephric kidney development. *bioRxiv* 2022. doi: <https://doi.org/10.1101/2022.07.01.497442>.
- 72) Ma Q, Battelli L, Hubbs AF. Multiorgan autoimmune inflammation, enhanced lymphoproliferation, and impaired homeostasis of reactive oxygen species in mice lacking the antioxidant-activated transcription factor Nrf2. *Am J Pathol* 2006; 168: 1960-1974.
- 73) Zheng H, Whitman SA, Wu W, Wondrak GT, Wong PK, Fang D, Zhang DD. Therapeutic potential of Nrf2 activators in streptozotocin-induced diabetic nephropathy. *Diabetes* 2011; 60: 3055-3066.
- 74) Aleksunes LM, Goedken MJ, Rockwell CE, Thomale J, Manautou JE, Klaassen CD. Transcriptional regulation of renal cytoprotective genes by Nrf2 and its potential use as a therapeutic target to mitigate cisplatin-induced nephrotoxicity. *J Pharmacol Exp Ther* 2010; 335: 2-12.
- 75) Nezu M, Souma T, Yu L, Suzuki T, Saigusa D, Ito S, Suzuki N, Yamamoto M. Transcription factor Nrf2 hyperactivation in early-phase renal ischemia-reperfusion injury prevents tubular damage progression. *Kidney Int* 2017; 91: 387-401.